ARTHRITIS & RHEUMATISM
Vol. 54, No. 11, November 2006, pp 3423–3432
DOI 10.1002/art.22178

Activation of Nitric Oxide Signaling by the Rheumatoid Arthritis Shared Epitope

Song Ling,[1] Angela Lai,[1] Olga Borschukova,[2] Paul Pumpens,[2] and Joseph Holoshitz[1]

Objective. **Susceptibility to rheumatoid arthritis (RA) is closely associated with *HLA–DRB1* alleles encoding a shared epitope (SE) in positions 70–74 of the HLA–DRβ chain. The mechanistic basis for this association is unknown. Given the proposed pathogenic role of nitric oxide (NO) in RA, this study was undertaken to examine whether the SE can trigger NO signaling events.**

Methods. **The intracellular levels of NO were measured with the fluorescent NO probe 4,5-diaminofluorescein diacetate and by the 2,3-diaminonaphthalene method. NO synthase activity was determined by measuring the rate of conversion of radioactive arginine to citrulline. Levels of cGMP were measured with a commercial enzyme-linked immunosorbent assay, and the cytolytic activity of T cells was measured using a standard ^{51}Cr release assay.**

Results. **Lymphoblastoid B cell lines carrying SE-positive HLA–DR alleles displayed a higher rate of spontaneous NO production compared with SE-negative cells. L cell transfectants expressing SE-positive DR molecules on their surface also generated higher levels of NO. Tetrameric HLA–DR molecules containing a DRβ-chain encoded by the SE-positive *DRB1*0401* allele stimulated fibroblast cells to produce higher levels of NO compared with cells stimulated with a control HLA–DR tetramer. Multimeric hepatitis B core proteins engineered to express region 65–79 encoded by the *DRB1*0401* allele, but not the same region encoded by the control allele *DRB1*0402*, stimulated NO production in fibroblasts. Similarly, synthetic 15-mer peptides corresponding to the region 65–79 encoded by SE-positive alleles triggered increased NO levels when incubated with class II major histocompatibility complex–negative cells. The signaling pathway was found to involve NO synthase activation, followed by increased production of cGMP. SE-triggered increased NO levels inhibited cytolytic elimination of target cells.**

Conclusion. **The SE can trigger NO-mediated signaling events in opposite cells, and may thereby contribute to RA pathogenesis.**

Rheumatoid arthritis (RA) is strongly associated with *HLA–DRB1* alleles encoding a 5–amino-acid sequence motif that is commonly referred to as the shared epitope (SE), in residues 70–74 of the DRβ-chain (1). The mechanism by which the SE increases susceptibility to RA is unknown. On the basis of the known role of class II major histocompatibility complex (MHC) molecules in antigen presentation, several hypotheses have been put forth to explain the mechanisms of action of SE-associated disease susceptibility, including presentation of arthritogenic self peptides (2), molecular mimicry with foreign antigens (3), and T cell repertoire selection (4). Although all of these hypotheses are plausible, they are difficult to reconcile with the fact that the supporting evidence for antigen-specific responses as the primary cause of RA is scant and inconsistent.

In addition to RA, several other human diseases have been shown to be associated with SE-encoding *DRB1* alleles, including polymyalgia rheumatica (5), giant cell arteritis (5), autoimmune hepatitis (6), erosive bone changes in psoriatic arthritis (7), and early-onset chronic lymphoid leukemia (8), among other diseases.

Dr. Holoshitz's work was supported by the NIH (grants AI-47331, AR-46468, and AR-20557), the Arthritis Foundation (Innovative Research Grant), and the University of Michigan Biotechnology Development Fund.

[1]Song Ling, PhD, Angela Lai, Joseph Holoshitz, MD: University of Michigan, Ann Arbor; [2]Olga Borschukova, Paul Pumpens, PhD: Biomedical Research and Study Center, University of Latvia, Riga, Latvia.

Drs. Ling and Holoshitz have a US patent for USPTO 7,074,893. Dr. Holoshitz receives licensing fees for an unrelated technology from Protein Design Laboratories through the Stanford Technology Office.

Address correspondence and reprint requests to Joseph Holoshitz, MD, Department of Internal Medicine, University of Michigan, 1150 West Medical Center Drive, 5520 MSRB I, Ann Arbor, MI 48109-0680. E-mail: jholo@umich.edu.

Submitted for publication April 4, 2006; accepted in revised form July 26, 2006.

Furthermore, the SE has been shown to be associated with spontaneous RA-like disease in dogs (9) and to facilitate collagen-induced arthritis (10) and experimental encephalomyelitis (11) in *HLA–DRB1*0401*–transgenic mice. Thus, the promiscuous association of SE-encoding *DRB1* alleles with pathogenically diverse diseases, with no apparent antigen or species specificity, suggests that in addition to its known role in antigen presentation, the SE may have non–antigen-specific effects.

In this study, we have undertaken to investigate the role of nitric oxide (NO) as a potential mediator of the SE effect, based on the following reasoning. NO is a ubiquitous signaling molecule with versatile effects in the immune system (for review, see ref. 12). Its proinflammatory effects in RA have been noted (13), as indicated by the significant correlation observed between increased NO levels and inflammatory markers of the disease (14). Furthermore, antirheumatic agents have been shown to suppress NO production (13,15). Excessive levels of NO, either alone or in conjunction with intercurrent oxidative challenges, can cause mutations (16), increase the risk of lymphoma (17), and accelerate telomere shortening (18), all of which are events that have been found in association with RA (19–21) or with the SE (22). Thus, multiple lines of evidence suggest that NO may be an important factor in RA and its association with the SE.

The findings of the present study indicate that cells carrying SE-positive *HLA–DRB1* alleles display increased constitutive NO production. Increased NO levels can also be seen in class II MHC–negative murine cells expressing human SE-positive DR molecules through complementary DNA (cDNA) transfection, indicating that the effect is not due to linkage disequilibrium with another gene. Synthetic proteins and peptides expressing the SE motif can mimic the signaling effect of the native DR molecule. We further show that SE-triggered NO signaling impedes cytolytic elimination of target cells. Thus, SE-positive HLA–DR molecules possess a unique ability to activate a biologically consequential, NO-mediated signaling pathway.

PATIENTS AND METHODS

Study subjects. Lymphoblastoid B cell lines from a total of 81 blood donors, including 11 pairs of RA-discordant monozygotic (MZ) twins (22 subjects) and 59 unrelated individuals, were used in this study. Twenty-seven donors had a diagnosis of RA, while 14 had other autoimmune diseases (including 6 patients with juvenile RA, 5 with type I diabetes, and 3 with autoimmune thyroiditis). Another group of 40 blood donors comprised the healthy control group. The RA group did not differ significantly from the healthy group demographically (no differences in the male-to-female ratio or mean age). Of the 81 donors, 52 carried 1 or 2 SE-positive *HLA–DRB1* alleles. The remaining 29 donors were SE-negative.

Cell lines, HLA–DR typing, and culture conditions. B lymphocyte lines, prepared from peripheral blood by Epstein-Barr virus transformation, were grown in supplemented RPMI 1640 medium. The cell lines were HLA–DR typed using commercial polymerase chain reaction–based, low–medium resolution DRB1 typing kits (Dynal Biotech, Brown Deer, WI), followed by high-resolution DRB1 allele–specific typing when indicated. The murine L cell transfectants expressing human HLA–DRα/β heterodimers were generated as described previously (23) and maintained in Dulbecco's modified Eagle's medium (DMEM) supplemented with 10 m*M* HEPES, 2 m*M* glutamine, 1% penicillin/streptomycin, 10% fetal calf serum, and 500 μg/ml G418. Human M1 fibroblasts were grown in DMEM containing 10% fetal bovine serum (FBS), penicillin/streptomycin, and 10 m*M* HEPES buffer solution. Synovial fibroblastoid cells were prepared from the synovial tissue of 1 RA patient, and then propagated in supplemented DMEM and used in passages 3–5. Human γ/δ T cell clones Tcc54 and Tcc62 were isolated and cultured as previously described (24). Human γ/δ T cell leukemia PEER cells were grown in RPMI 1640 medium supplemented with 10% FBS, penicillin/streptomycin, and 10 m*M* HEPES buffer solution.

Synthesis and solid-phase immobilization of peptides. Peptides were synthesized at the University of Michigan Protein Structure Facility (Ann Arbor) on a Rainin PTI Synphony automated peptide synthesizer. Each residue was coupled twice with 200 m*M* HOBt plus HBTU and 400 m*M* *N*-methylmorpholine for 60 minutes, and capped with 50% acetic anhydride in dimethylformamide. The resins used were Fmoc-PAL-PEG resins from Applied Biosystems (Foster City, CA). Peptides were purified to >90% by high-performance liquid chromatography. All peptides were C- and N-terminally blocked. The sequences of the four 15-mer peptides used, along with their corresponding *DRB1* alleles, are shown in Table 1.

To immobilize peptides on a solid phase, cyanogen bromide–activated Sepharose 4B beads were washed with 1 m*M* HCl and incubated overnight at 4°C with peptides in buffer containing 0.1*M* $NaHCO_3$ and 0.5*M* NaCl (pH 8.0). Five milligrams of peptide was mixed with 1 ml of Sepharose 4B beads. Free Sepharose groups were blocked with 0.2*M* glycine (pH 8.0) for 2 hours at room temperature. Columns were washed at 4°C with buffer containing 0.1*M* $NaHCO_3$ and 0.5*M* NaCl (pH 8.0), followed with 0.5*M* CH_3COONa (pH 4.0) buffer, and finally with phosphate buffered saline (PBS) at pH 7.5. The efficiency of binding was determined by quantification of the residual concentration of peptides in buffer, after overnight incubation with the beads.

NO quantification. To determine the rate of NO production in lymphoblasts, cells were first loaded with 20 μM of the fluorescent NO probe 4,5-diaminofluorescein diacetate (DAF-2DA) and then incubated in the dark at 37°C for 1 hour, washed, and plated at a density of 1×10^5 per well in 96-well plates (OptiPlate; PerkinElmer Life Sciences, Wellesley, MA) in 100 μl of DMEM/phenol red–free medium. The fluores-

Table 1. Peptides used in the study

Designation	Amino acid sequence	Encoding *HLA–DRB1* alleles
65-79*0401	KDLLEQKRAAVDTYC	**0401; *0413; *0416; *0421; *1419; *1421*
65-79*0402	KDILEDERAAVDTYC	**0402; *0414; *0103; *1102; *1116; *1120; *1121; *1301; *1302; *1304; *1308; *1315; *1317; *1319; *1322; *1416*
65-79*0403	KDLLEQRRAEVDTYC	**0403; *0406; *0407; *0417; *0420*
65-79*0404	KDLLEQRRAAVDTYC	**0404; *0405; *0408; *0410; *0419; *0101; *0102; *1402; *1406; *1409; *1413; *1417; *1420*

cence level was recorded every 5 minutes over a period of 500 minutes, using a Fusion αHT system (PerkinElmer Life Sciences) at an excitation wavelength of 488 nm and emission wavelength of 515 nm. The NO production rate is expressed as the mean ± SEM fluorescence units per minute.

The rate of NO production in adherent cells was determined in the same way as that for lymphoblasts, with the exception that cells were first plated overnight at a density of 3×10^4 per well in flat-bottom, 96-well plates (Costar, Cambridge, MA). The resultant subconfluent monolayer cultures were loaded with DAF-2DA. The NO production rates were then determined as described above.

To quantify NO levels directly, cell culture medium was changed to NO assay buffer (20 m*M* Tris, 100 m*M* NaCl, 0.1 m*M* EDTA [pH 7.6]). At different time points, supernatants were collected and spun down to remove cell debris. Nitrate was first transformed to nitrite by incubation with nitrate reductase for 60 minutes at room temperature. Subsequently, 2,3-diaminonaphthalene was added, and fluorescence of 2,3-naphthotriazole was measured using the Fusion αHT system, with an excitation wavelength at 375 nm and emission wavelength at 415 nm.

Measurement of NO synthase (NOS) activity. NOS activity was determined in intact M1 cells by measuring the conversion of radioactive L-arginine to radioactive L-citrulline. M1 cells were incubated in 6-well plates at 10^6 cells per well with HEPES buffer (10 m*M* HEPES, pH 7.4, 145 m*M* NaCl, 5 m*M* KCl, 1 m*M* $MgCl_2$, 10 m*M* glucose, with or without L-N^G-nitroarginine methyl ester) for 20 minutes at 37°C. Five minutes prior to cell stimulation with peptides, 2 μCi/ml radioactive L-arginine was added. The NOS reaction was stopped at different time points thereafter by adding ice-cold PBS with 4 m*M* EDTA and 5 m*M* L-arginine. Cells were then subjected to freeze-thawing once on dry ice, and 100% cold ethanol was added for extraction. Cells were left to evaporate before addition of 1 ml of 10 m*M* HEPES (pH 5.5). Fifty microliters was withdrawn to check the total incorporation of radioactive L-arginine. The remaining volume was loaded on the cation retention column AG50WX8 to separate radioactive L-citrulline from radioactive L-arginine. The radioactive L-citrulline was then quantified by scintillation counting.

Measurement of cGMP. The levels of cGMP were measured using an enzyme-linked immunosorbent assay kit (Amersham Biosciences, Uppsala, Sweden) according to the manufacturer's instructions. Cells were cultured in 96-well plates, and then lysed by addition of 5% dodecyltrimethyl ammonium bromide.

Cytotoxicity assays. Cytolysis of B cell targets by γ/δ T cells was performed using a standard ^{51}Cr release assay. Specific lysis was calculated as described previously (25).

HLA–DR tetramers. Tetramers DRB1*0401/DRA1*0101 (designated herein as T-DRB1*0401) and DRB1*1501/DRA1*0101 (designated T-DRB1*1501) containing the class II–associated invariant chain peptide in the antigenic groove were generated at the National Institutes of Health Tetramer Facility, using previously described methods (26).

Generation of chimeric hepatitis B core (HBc) particles expressing the allelic third hypervariable region (HVR3) of DRβ. The vector p2-19, which expresses C-terminally shortened HBcΔ (lacking the C-terminal region 145–183 [27]), was chosen for peptide display between HBc amino acid residues 78 and 79. The following oligonucleotides were synthesized, annealed, and inserted into the HBc gene after cleavage with restriction enzymes *Eco* 72I and *Eco* 105I: for *HLA–DRB1*0401* HVR3 (65-KDLLEQKRAAVDTYC-79), 5′-AAAGATCTTCTAGAACAAAAAAGAGCTGCAGTCGACACATATTGT-3′ and 5′-ACAATATGTGTCGACTGCAGCTCTTTTTTGTTCTAGAAGATCTTT-3′, and for *HLA–DRB1*0402* HVR3 (65-KDILEDERAAVDTYC-79), 5′-AAAGATATTCTAGAAGATGAAAGAGCTGCAGTCGACACTTATTGT-3′ and 5′-ACAATAAGTGTCGACTGCAGCTCTTTCATCTTCTAGAATATCTTT-3′.

The K802 (hsdR, gal, met, supE, mcrA, mcrB) strain of *Escherichia coli* was used to produce chimeric HBc derivatives. The cells were lysed by a 30-minute incubation on ice in lysis buffer containing 50 m*M* Tris HCl (pH 8.0), 50 m*M* EDTA, 100 μg/ml phenylmethylsulfonyl fluoride, and 2 mg/ml lysozyme, and then frozen and thawed twice, after which 10 m*M* $MgCl_2$ and 20 μg/ml DNase were added. After ultrasonication (22 kHz), protein lysate was centrifuged at low speed, and the protein was precipitated from the supernatant with ammonium sulfate at 30% saturation for 12 hours at 4°C. Pellets were resuspended in PBS buffer, containing 0.5% Triton X-100 and 0.3–0.6*M* urea. Five microliters of protein was loaded onto a Sepharose CL4B column (2.5 × 85 cm) and eluted with PBS buffer with 0.15–0.3*M* urea. Fractions containing HBc recombinant proteins, as confirmed by polyacrylamide gel electrophoresis, were pooled and concentrated by ammonium sulfate precipitation at 50% saturation. Pellets were resuspended in PBS, dialyzed overnight against 1,000 volumes of the same buffer, and stored in 50% glycerol at −20°C. The quality of the capsid preparations was checked by electron microscopy.

Statistical analysis. Unless stated otherwise, Student's *t*-test was used for group comparisons, with statistical significance defined as a *P* value less than 0.05. All results are expressed as the mean ± SEM. Dose-response curves and calculation of the 50% inhibitory concentration (IC_{50}) were determined using PRISM 3.0 software (GraphPad Software, San Diego, CA).

RESULTS

To ascertain whether the presence of the SE affects NO signaling, we compared spontaneous NO production in B lymphocyte lines from 44 HLA–DR–typed individuals. Cells were loaded with the fluorescent NO probe DAF-2DA and were cultured over a set time course at high density to allow close cell–cell contact.

As can be seen in Figures 1A–C, although constitutive NO production was seen in all lines, SE-positive cells exhibited a much higher rate of NO production. Curves for 2 representative cell lines are shown, to illustrate the difference between SE-positive and SE-negative cells (Figure 1A). The mean NO production rate was significantly higher in the SE-positive group compared with the SE-negative group ($P = 0.0008$) (Figure 1B). Direct measurement of NO levels (Figure 1C) confirmed that SE-positive cells produced significantly more NO than SE-negative cells ($P = 8.7 \times 10^{-6}$). No significant difference in NO production was found between healthy individuals and RA patients within the SE-positive group, suggesting that the SE rather than RA is responsible for the accelerated NO production.

To more conclusively determine the relative roles of RA and the SE, we analyzed 11 pairs of SE-positive, RA-discordant MZ twins. No significant difference in the rate of NO production was found between the RA twins and their healthy cotwins (Figure 1D). Thus, spontaneous NO overproduction is an SE-associated rather than RA-associated aberration.

To determine whether NO overproduction could be attributed to the *DRB1* gene itself or whether it was the result of another gene secondary to linkage disequilibrium, we studied murine L cell transfectants expressing human HLA–DRα/β heterodimers on their surface (23). As can be seen in Figure 1E, L565.5 cells expressing the SE-positive allele *DRB1*0401* showed higher spontaneous production of NO than did L514.3 transfectants expressing the SE-negative allele *DRB1*0402*.

To investigate whether the DR molecule is directly involved, we used SE-positive and SE-negative HLA–DR tetramers. The assembly of class II MHC tetrameric molecules depends on the presence of an antigenic groove peptide, which should conform to a distinct sequence motif for each allele. To allow comparisons between the SE-negative and SE-positive tetramers independent of allele-specific groove peptides, we used tetramers containing a covalently bound CLIP peptide (26). To determine the signaling activity of these tetramers, we used class II HLA–negative human M1 fibroblasts. In contrast to lymphoblasts, these adherent cells are grown sparsely in subconfluent monolayers and display low rates of spontaneous NO production (results not shown).

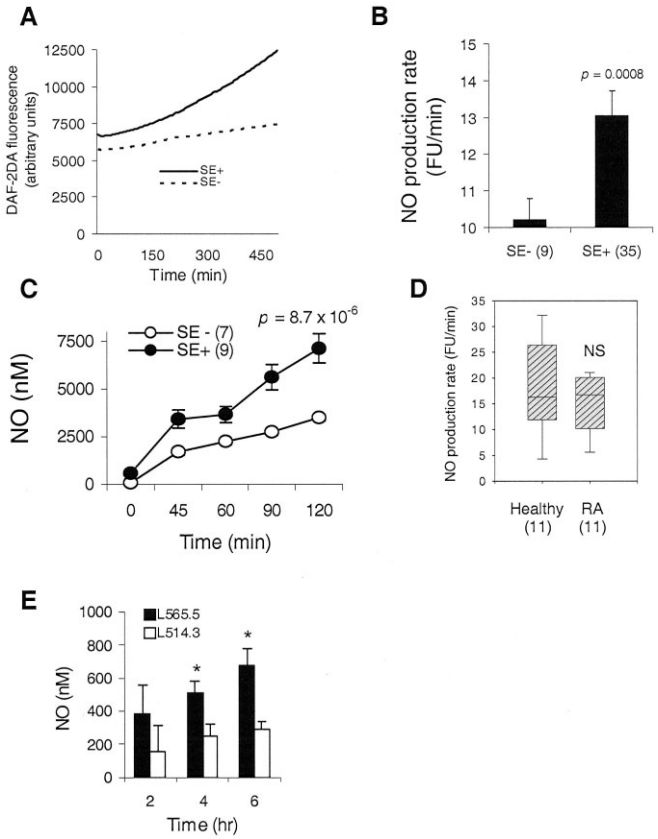

Figure 1. Increased nitric oxide (NO) levels in shared epitope (SE)–expressing cells. **A,** Representative time-course curves of NO production, measured as fluorescence with the NO probe 4,5-diaminofluorescein diacetate (DAF-2DA) in SE-positive and SE-negative B lymphocyte cell lines. **B,** Spontaneous NO production by B lymphocytes in the SE-positive and SE-negative groups, compiled from 3 consecutive experiments in each cell line. **C,** NO production rates in B lymphocytes in the SE-positive and SE-negative groups, compiled from 3–5 consecutive experiments in each cell line. **D,** Analysis of NO production rates in 11 pairs of rheumatoid arthritis (RA)–discordant monozygotic twins. **E,** Spontaneous production of NO over time in murine L cell transfectants expressing cDNA corresponding to either *DRB1*0401* (L565.5) or *DRB1*0402* (L514.3). $*$ = $P < 0.05$ versus L514.3 cells at the respective time points, by paired *t*-test. Numbers in parentheses in **B–D** are the number of donors in each group. Values in **B, C,** and **E** are the mean ± SEM. Values in **D** are box plots, with lines in the boxes indicating the median, the boxes representing the 25th and 75th percentiles, and lines outside the boxes representing the 10th and 90th percentiles. FU = fluorescence units; NS = not significant.

As shown in Figure 2A, M1 fibroblasts stimulated with the SE-positive T-DRB1*0401 tetramer generated significantly more NO compared with cells stimulated

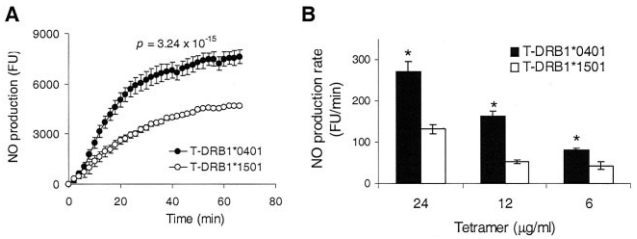

Figure 2. Triggering of NO production by SE-expressing HLA–DR tetrameric molecules. **A,** DAF-2DA fluorescence (in FU) was determined over time in human M1 fibroblasts incubated with 24 μg/ml of corticotropin-like intermediate lobe–containing tetramers of the SE-positive allele *DRB1*0401* (T-DRB1*0401) or a control, SE-negative allele *DRB1*1501* (T-DRB1*1501). Values are the mean ± SEM fluorescence in triplicate wells. **B,** Dose-response of T-DRB1*0401–triggered NO production in M1 cells. Values are the mean ± SEM FU/minute above control levels in triplicate wells. $* = P < 0.05$ versus control tetramer at each dose. See Figure 1 for other definitions.

with the SE-negative T-DRB1*1501 control tetramer ($P = 3.24 \times 10^{-15}$). Because T-DRB1*0401 and T-DRB1*1501 share identical DRβ-chains and groove peptides, their differential signaling activity can only be attributed to their distinct DRβ-chains. Results of the dose-response analysis with the 2 tetramers are shown in Figure 2B. The IC_{50} calculations for T-DRB1*0401 (not shown) revealed an IC_{50} value of $\sim 3.0 \times 10^{-8} M$. Thus, tetramer T-DRB1*0401 is a specific and potent stimulator of NO production.

The DRβ-chains encoded by the *DRB1*0401* and *DRB1*1501* alleles differ from each other by 13 amino acid residues, spread throughout the molecule. Therefore, we proceeded to better map the active region on the DRβ-chain. Given the promiscuous association of the SE with pathogenically diverse diseases and with no apparent antigen or species specificity, we hypothesized that the "naked" SE-carrying α-helical loop, independent of any antigenic groove peptide, is responsible for the aberration. To generate a protein expressing the naked α-helical SE-positive region in its native conformation, we genetically engineered the HVR3 (residues 65–79) encoded by SE-positive or SE-negative *DRB1* alleles into the spikes of a recombinant HBc protein capsid. HBc capsids are efficient nonreplicative and noninfective carriers of foreign epitopes (28). Importantly, the tips of each spike form α-helical structures, thus mimicking the native conformation of the HVR3.

Oligonucleotides encoding residues 65–79 of either the SE-positive allele *DRB1*0401* or the SE-negative allele *DRB1*0402* were inserted into the p2-19 vector between codons 78 and 79, at the tips of the HBc spikes (Figures 3A–C). As can be seen, SE-positive HBc chimeric capsids (designated HBc*0401), but not the SE-negative capsids (HBc*0402), triggered rapid NO production (Figure 3D). The HVR3 encoded by these 2 alleles differs by 3 amino acid residues, thus suggesting that the active site can be mapped to the HVR3 region.

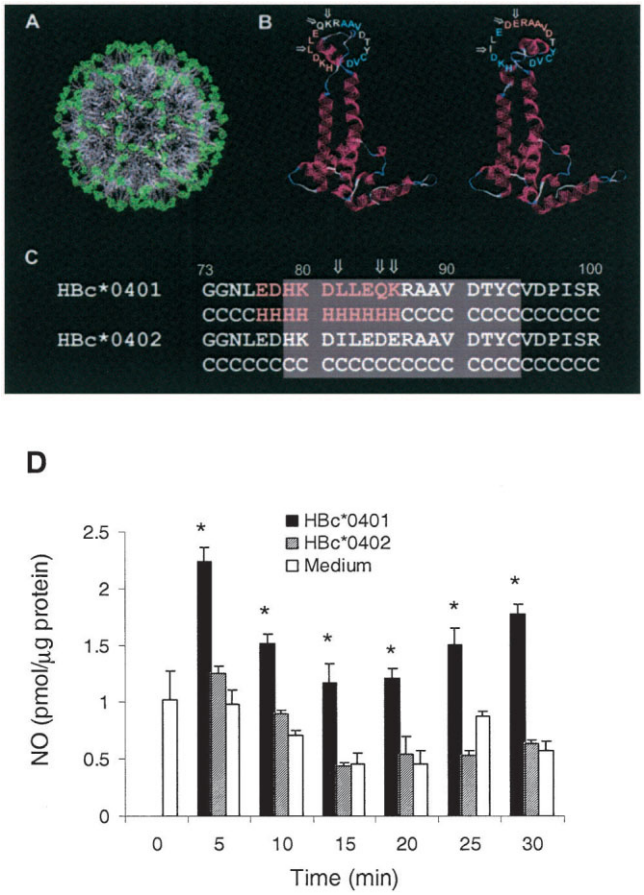

Figure 3. Triggering of NO production by third hypervariable region–expressing chimeric hepatitis B core (HBc) capsids. **A,** A radiographically based, 3-dimensional (3-D) presentation of the HBc*0401 shell, calculated on the basis of the HBc carrier radiographic data (T = 4, resolution 3.3Å) using the 3-D JIGSAW and VIPER programs. The inserted sequence is in green. **B,** A radiographically based, computed presentation of the fold of the HBc*0401 (left) and HBc*0402 (right) monomers, as predicted by the 3-D JIGSAW program. The amino acid sequences at the HBc monomer tips are presented by 1-letter codes. **Arrows** denote amino acid differences between HBc*0401 and HBc*0402. **C,** A linear presentation by 3-D PSSM prediction analysis of the fold containing the SE insertions (gray-shaded areas) with the immediately adjacent HBc residues. The α-helices are in red, coils are in white, and β-turns are in blue. **Arrows** denote amino acid differences between HBc*0401 and HBc*0402. **D,** NO levels over time in human γ/δ T cell leukemia PEER cells incubated with 2.5 μg/ml of either HBc*0401 or HBc*0402 or with medium alone. Values are the mean and SEM. $* = P < 0.05$ versus HBc*0402 and medium alone at the respective time points. See Figure 1 for other definitions.

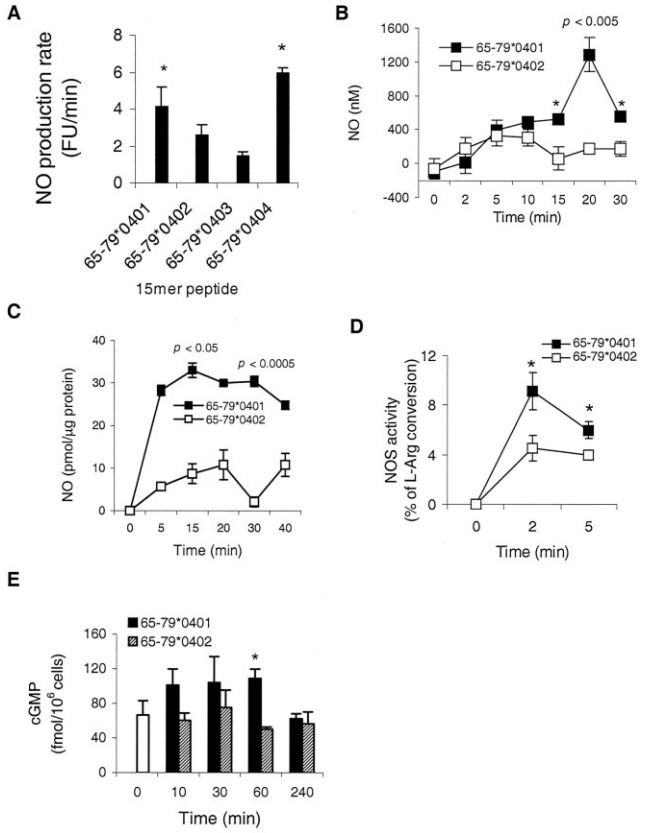

Figure 4. Triggering of NO production by SE-expressing 15-mer peptides. **A,** NO production rates (in FU/minute for DAF-2DA fluorescence) in M1 fibroblasts stimulated with 50 μg/ml of soluble 15-mer synthetic peptides. **B,** NO production in human fibroblast M1 cells incubated with Sepharose bead–immobilized peptides 65–79*0401 or 65–79*0402. **C,** NO levels in human RA synoviocytes incubated with Sepharose bead–immobilized peptides 65–79*0401 or 65–79*0402. **D,** NO synthase (NOS) activity (measured as the percent of L-arginine [L-Arg] conversion) in human M1 fibroblasts at different time points following incubation with Sepharose bead–immobilized peptides 65–79*0401 or 65–79*0402. **E,** Levels of cGMP in M1 cells at different time points following exposure to Sepharose bead–immobilized SE-positive peptide 65–79*0401 or control SE-negative peptide 65–79*0402. Levels in untreated cells at time 0 are indicated by an open bar. Values are the mean ± SEM in triplicate cultures. $* = P < 0.05$ versus comparator peptide(s) at the individual time points. See Figure 1 for other definitions.

These results also indicate that SE-carrying α-helical loops, independent of any antigenic groove peptide, can trigger NO signaling.

NO signals could also be triggered by soluble synthetic peptides containing the SE sequence (Figure 4A). Cells preincubated with SE-positive 15-mer peptides corresponding to the HVR3 of the SE-positive *DRB1* alleles **0401* (designated 65-79*0401) or **0404* (designated 65-79*0404) triggered significantly higher NO production rates in M1 cells compared with that by control peptides corresponding to the HVR3 of the SE-negative *DRB1* alleles **0402* or **0403* (designated 65–79*0402 and 65–79*0403, respectively) (Figure 4). Time-course analysis of the SE peptide–triggered NO production in human fibroblastoid cells (Figure 4B) showed a response within 15–30 minutes after incubation.

SE-triggered NO signaling could be seen in diverse lineages, including human B lymphoblastoid cells (Figure 1), human fibroblasts (Figures 4A and B), RA synoviocytes (Figure 4C), human γ/δ T cell leukemia PEER cells (Figure 3D), human neuroblastoma cells (results not shown), and murine fibroblasts (Figure 1E). SE-triggered NO production was found to be mediated by rapid activation of NOS (Figure 4D), followed by increased levels of cGMP (Figure 4E).

Among its many effects, NO has been previously shown to inhibit apoptotic target killing by cytotoxic T cells (29,30). Since impaired apoptotic elimination of autoreactive cells has been proposed as a triggering event in RA (31,32), we investigated whether the SE might be a contributing factor. To that end, we have studied apoptotic target killing by T cell clones expressing the $V_\gamma 9/V_\delta 2$ receptors. These very potent, non–MHC-restricted killer cells play an immune surveillance role (33) and it has been previously proposed that they play a protective role in RA by eliminating autoreactive cells (34,35).

As can be seen in Figure 5A (HLA typing information is available from the authors on request),

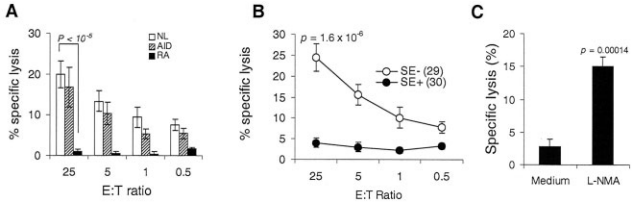

Figure 5. Modulation of T cell–mediated cytolysis by the shared epitope (SE). **A,** Cytolytic potency of cloned $V_\gamma 9/V_\delta 2$ T cells against 59 HLA–DR–typed B cell line targets (from 29 healthy subjects [NL], 16 patients with rheumatoid arthritis [RA], and 14 patients with other autoimmune diseases [AID]). **B,** Comparison of susceptibility to cytolysis by $V_\gamma 9/V_\delta 2$ T cells of targets from SE-negative and SE-positive donors. The numbers of donors are shown in parentheses. **C,** Resistance of SE-positive targets to T cell–induced cell death mediated by nitric oxide. Five SE-positive target cell lines were cultured for 96 hours prior to the assay with or without 5 m*M* of N^G-monomethyl-L-arginine (L-NMA). At the end of the culture period, cells were washed extensively and used as targets for $V_\gamma 9/V_\delta 2$ effector cells at an effector cell to target cell (E:T) ratio of 10. Values are the mean ± SEM.

analysis of the susceptibility to γ/δ T cell–mediated apoptotic killing of lymphoblastoid B cell targets from 59 individuals (29 healthy subjects, 16 patients with RA, and 14 patients with other autoimmune diseases) revealed no significant difference between healthy subjects and those with other autoimmune diseases; however, a highly significant ($P < 10^{-5}$) difference was seen between healthy subjects and RA patients (Figure 5A). When the SE-negative and SE-positive groups were compared, a highly significant ($P = 1.6 \times 10^{-6}$) resistance to apoptosis was seen in SE-positive targets (Figure 5B). Thus, in the presence of SE-positive targets, the highly potent γ/δ T cells are rendered completely unresponsive.

Since RA and the SE are closely associated, we assessed whether the patient groups differed according to disease status or to SE status. To that end, a two-factor full-factorial analysis of variance was used. There was no interaction between diagnostic group and SE status, and the groups did not differ by diagnosis. In contrast, the effect of being SE positive was significant ($P = 0.015$).

In another approach, hierarchical regression modeling was used, in which diagnosis was first forced into the model and then SE status was entered, in order to account for any remaining variance above what could be known by diagnosis alone. The prediction model of susceptibility to apoptotic death based on disease category alone was not significant and accounted for only 3% of the variance. However, adding SE status to the model significantly improved its predictive ability, with an additional 35% of the variance being accounted for by SE status ($P < 0.001$). Taken together, these findings indicate that the SE status, rather than the diagnosis, is the main determining factor in susceptibility of target cells to γ/δ T cell apoptotic killing. Resistance to T cell–induced apoptotic target killing in SE-positive cells could be reversed by preincubation with the NOS inhibitor N^G-monomethyl-L-arginine, indicating that the resistance was due to increased NO production (Figure 5C).

DISCUSSION

Our results demonstrate that the SE can trigger NO-mediated signaling events in opposite cells. The NO pathway is constitutively active in cells carrying SE-encoding *DRB1* alleles and in class II MHC–negative L cells transfected with SE-encoding *DRB1* cDNA. The pathway can also be activated in class II MHC–negative cells by SE-expressing HLA–DR tetramers, by multimeric recombinant proteins engineered to express the SE sequence, and by short synthetic peptides expressing the SE motif.

The SE has long been known to have an association with susceptibility to RA. However, due to the paucity of experimental evidence of direct SE-mediated biologic effects, a recurring question has been whether the SE–RA association is due to the *DRB1* itself or is secondary to putative linkage disequilibrium with another gene (36). By using L cell transfectants that are expressed on the surface of different *DRB1*-encoded molecules, we have herein demonstrated that the *DRB1* gene is directly responsible for a signaling aberration in an allele-specific manner. To the best of our knowledge, these findings provide the first direct evidence that the SE itself exerts an allele-specific functional aberration independent of antigen presentation.

Our data indicate that conformationally intact SE-positive HLA–DR molecules can activate NO-mediated signaling in their cell surface–expressed and tetrameric cell–free form. It should be pointed out that in 2 experiments, SE-negative tetramers triggered some NO production (Figure 2), and SE-negative Sepharose-immobilized peptides triggered weak NOS responses (Figure 4D) in M1 cells. Importantly, however, these responses were significantly lower than those triggered by the respective SE-positive ligands and were likely nonspecific. Consistent with this assessment, MHC tetramers have been previously shown to display nonspecific binding activity (37). Furthermore, our recent data strongly suggest that these rare and weak responses are biologically nonconsequential. Neither the T-DRB1*1501 tetramer nor the Sepharose bead–immobilized SE-negative peptides were able to activate functional downstream signaling events that SE-bearing reagents characteristically trigger (Ling S, Holoshitz J: unpublished observations). Thus, although SE-negative molecules can trigger some nonspecific NO responses in rare experimental circumstances, these responses differ both quantitatively and qualitatively from those triggered by SE-positive ligands.

The effect of the native SE could be reproduced by recombinant multimeric protein particles engineered to express the SE motif in its α-helical conformation, and by short synthetic peptides corresponding to the HVR3 of the DRβ-chain (residues 65–79). It is noteworthy that synthetic peptides corresponding to the region 65–79 of the DQα-chain have been previously reported to exert signaling events in lymphoid cells (38). However, that effect was non–allele-specific and was dependent on intracellular interference with the cell

cycle machinery. In contrast, the SE peptides operate at the cell surface and their effect is allele-specific.

In this study, we investigated 2 SE-positive 15-mer peptides expressing a core sequence of QKRAA or QRRAA. These sequences correspond to at least 19 *HLA–DRB1* alleles (see Table 1), which are found in the vast majority of RA patients. A small minority of RA patients carry allele *DRB1*1001*, with a core sequence of ^{70}RRRAA^{74}. Using another experimental system to assess SE-mediated signaling aberrations, we recently confirmed (Ling S, et al: unpublished observations) that synthetic peptides expressing the *DRB1*1001*-encoded SE motif share functional activities with the peptides described herein. In addition, among the 44 B cell lines used for NO production studies, there was 1 cell line carrying the *DRB1*1001*. This B cell line showed one of the highest NO production rates (results not shown). Thus, the findings described herein with peptides corresponding to the 2 common SE sequences, QKRAA and QRRAA, suggest the presence of a functional property that is shared by the entire array of *DRB1* SE-positive alleles.

Short synthetic peptides are generally expected to assume a random conformation in solution. Therefore, it is likely that only a small minority of the peptidic molecules in our studies presented the native SE α-helical conformation at any given time. Consistent with this assessment, T-DRB1*0401 tetramers, which preserve the native conformation of the DR molecule, and HBc*0401 capsids, in which the inserted SE region assumes a stable α-helical conformation, were both at least 200-fold more potent, on a molar basis, than the corresponding soluble SE-expressing 15-mer peptide (Ling S, et al: unpublished observations). More importantly, our experiments with intact cells indicate that the SE is acting as a ligand in physiologic settings.

In its native conformation, the SE occupies ~1.5 α-helical loops in the center of the DRβ1 domain and builds the lateral wall of the fourth pocket of the peptide-binding groove. Although this region is thought to be dedicated to antigen presentation, careful review of the region 70–74 in radiographic crystallography maps (39) reveals a sizable gap between the collective electron densities of groove-bound antigenic peptides and the van der Waals surface at the region 70–74 of the DRβ-chain. Thus, the SE represents a relatively free protrusion in the DRβ-chain, which, depending on the level of antigenic peptide occupancy and the nature of that peptide, could allow sufficient room for interaction with other molecules. This scenario is reminiscent of the signaling role played by discrete α-helical loops in the class I MHC α2 domain (40,41), which is remarkably similar in its conformation to the DRβ1 domain (39).

The class I MHC α2 domain binds, in trans, to killer immunoglobulin-like receptors and modulates natural killer (NK) cell activity (41). Similar engagements exist between the nonclassic human class I MHC molecule HLA–E and the heterodimeric NKG2/CD94 receptor, and between MHC-like proteins, such as MICA and NKG2D. In addition, an α2 ligand on the human class I–like molecule HFE binds, in cis, to, and activates signal transduction through, the transferrin receptor (42), and a ligand in the α2 domain of murine M1 and M10 class Ib MHC molecules activates the pheromone receptor V2R in cis (43). Thus, there is ample evidence that discrete MHC α-helical loops can act as signal transduction ligands.

The present study findings suggest that the SE may be functioning in a manner reminiscent of the physiologic function of class I α2 domain ligands. However, unlike class I ligands, which act in an allele-promiscuous manner, the SE demonstrates exquisite allele specificity, as exemplified by the failure of 15-mer peptides corresponding to the HVR3 of *DRB1*0403*-encoded DR molecules to trigger NO signaling. Synthetic peptides corresponding to the same region encoded by allele *DRB1*0404*, which differ by a single amino acid residue (A74 in *DRB1*0404* versus E74 in *DRB1*0403*) were able to transduce a potent signal (Figure 4A). Whether SE-encoding *DRB1* alleles have preserved an ancestral functional trait that is shared with class I MHC molecules or whether the SE is an aberrant motif acquired accidentally during allelic diversification, and whether that motif mimics a physiologic ligand, is unknown.

These findings could invoke a new model explaining the events leading to onset of RA. According to this model, chronically increased NO levels, perhaps in conjunction with recurrent daily oxidative stresses, could create an environment conducive to the emergence of disease-initiation events. Consistent with this concept, a gene–environment interaction between the SE and smoking has been recently reported, with a 21-fold increased relative risk of RA-specific immune aberrations in smokers carrying 2 copies of the SE compared with SE-negative nonsmokers (44).

One potential SE-triggered, disease-initiating event could be an NO-induced epigenetic drift. Based on the very high discordance rate of RA observed in MZ twins (45), it has long been proposed that whereas

genetic factors play a major role in susceptibility to RA, disease onset may depend on nongenetic or epigenetic factors. NO has been previously shown to affect DNA methylation (46), accelerate telomere shortening (18), and increase epigenetic events (47). It could therefore contribute to an accelerated epigenetic drift in SE-positive individuals, as exemplified in recent telomere attrition studies (22). The cumulative and stochastic nature of such putative SE-driven epigenetic drifts could provide a plausible explanation for the delayed onset of RA and its seemingly random occurrence among genetically susceptible individuals, as well as the association of the SE with other diseases.

Beyond its potential role in disease onset, SE-triggered NO production could also contribute to RA pathogenesis through its proinflammatory effects. The roles of NO in the immune system are multiplex. Particularly relevant to RA are the known immunomodulatory effects of NO on dendritic cells, NK cells, and T and B lymphocytes. Increased NO levels can also lead to T cell hyporesponsiveness and resistance to apoptosis (for review, see ref. 12), which are aberrations that have been previously noted in RA (31,32,48). In this report, we present data exemplifying one candidate immune aberration caused by SE-triggered NO signaling. We demonstrate that SE-positive cells are conspicuously resistant to cytolytic elimination by $V_\gamma 9/V_\delta 2$ T cells. The resistance could be overcome by preincubating the targets with an NOS inhibitor. Statistical analysis revealed that the resistance was directly related to the SE, independent of the disease origin of the cells.

Finally, it should be noted that although the SE–RA association is consistently found across many ethnic groups, 5–10% of all RA patients, particularly African Americans (49), are SE-negative. Therefore, the possibility that NO-mediated, disease-causing aberrations could be triggered by SE-independent mechanisms merits consideration. It should also be noted that although this study demonstrated direct involvement of the SE in an RA-relevant functional aberration, whether and to what extent demographic factors, disease subsets, or clinical features affect the response, or its consequences, remain unknown. Likewise, this study does not compare the effect of different SE sequences (i.e., QKRAA versus QRRAA or RRRAA) or the effect of different haplotype contexts, nor does it address the role of single- versus double-SE gene dose or the effect of RA-protective DRB1 alleles (50). The answers to these and many other questions await further studies.

ACKNOWLEDGMENTS

We thank Dr. Mongshang Lin for expert technical assistance and advice during the process of this work, Dr. Indulis Gusars and Dr. Vijay Reddy for excellent mathematical modeling advice, Steven Knowlton for editorial assistance, Dr. David Williams for statistical advice, and Dr. Robert Karr for his generous gift of L cell transfectants. We also thank the National Institutes of Health Tetramer Facility for providing the HLA–DR tetrameric molecules.

REFERENCES

1. Gregersen PK, Silver J, Winchester RJ. The shared epitope hypothesis: an approach to understanding the molecular genetics of susceptibility to rheumatoid arthritis. Arthritis Rheum 1987;30: 1205–13.
2. Wucherpfennig KW, Strominger JL. Selective binding of self peptides to disease-associated major histocompatibility complex (MHC) molecules: a mechanism for MHC-linked susceptibility to human autoimmune diseases. J Exp Med 1995;181:1597–601.
3. La Cava A, Nelson JL, Ollier WE, MacGregor A, Keystone EC, Thorne JC, et al. Genetic bias in immune responses to a cassette shared by different microorganisms in patients with rheumatoid arthritis. J Clin Invest 1997;100:658–63.
4. Bhayani HR, Hedrick SM. The role of polymorphic amino acids of the MHC molecule in the selection of the T cell repertoire. J Immunol 1991;146:1093–8.
5. Weyand CM, Hunder NN, Hicok KC, Hunder GG, Goronzy JJ. HLA–DRB1 alleles in polymyalgia rheumatica, giant cell arteritis, and rheumatoid arthritis. Arthritis Rheum 1994;37:514–20.
6. Doherty DG, Donaldson PT, Underhill JA, Farrant JM, Duthie A, Meili-Vergani G, et al. Allelic sequence variation in the HLA class II genes and proteins in patients with autoimmune hepatitis. Hepatology 1994;19:609–15.
7. Korendowych E, Dixey J, Cox B, Jones S, McHugh N. The influence of the HLA-DRB1 rheumatoid arthritis shared epitope on the clinical characteristics and radiological outcome of psoriatic arthritis. J Rheumatol 2003;30:96–101.
8. Dorak MT, Machulla HK, Hentschel M, Mills KI, Langner J, Burnett AK. Influence of the major histocompatibility complex on age at onset of chronic lymphoid leukaemia. Int J Cancer 1996; 65:134–9.
9. Ollier WE, Kennedy LJ, Thomson W, Barnes AN, Bell SC, Bennett D, et al. Dog MHC alleles containing the human RA shared epitope confer susceptibility to canine rheumatoid arthritis. Immunogenetics 2001;53:669–73.
10. Rosloniec EF, Brand DD, Myers LK, Whittington KB, Gumanovskaya M, Zaller DM, et al. An HLA-DR1 transgene confers susceptibility to collagen-induced arthritis elicited with human type II collagen. J Exp Med 1997;185:1113–22.
11. Forsthuber TG, Shive CL, Wienhold W, de Graaf K, Spack EG, Sublett R, et al. T cell epitopes of human myelin oligodendrocyte glycoprotein identified in HLA-DR4 (DRB1*0401) transgenic mice are encephalitogenic and are presented by human B cells. J Immunol 2001;167:7119–25.
12. Bogdan C. Nitric oxide and the immune response. Nat Immunol 2001;2:907–16.
13. Stichtenoth DO, Frolich JC. Nitric oxide and inflammatory joint diseases. Br J Rheumatol 1998;37:246–57.
14. Yki-Jarvinen H, Bergholm R, Leirisalo-Repo M. Increased inflammatory activity parallels increased basal nitric oxide production and blunted response to nitric oxide in vivo in rheumatoid arthritis. Ann Rheum Dis 2003;62:630–4.
15. Wang B, Ma L, Tao X, Lipsky PE. Triptolide, an active component of the Chinese herbal remedy Tripterygium wilfordii Hook F,

inhibits production of nitric oxide by decreasing inducible nitric oxide synthase gene transcription. Arthritis Rheum 2004;50: 2995–3003.
16. Grant DD, Goldstein R, Karsh J, Birnboim HC. Nitric oxide donors induce large-scale deletion mutations in human lymphoblastoid cells: implications for mutations in T-lymphocytes from arthritis patients. Environ Mol Mutagen 2001;38:261–7.
17. Tamir S, de Rojas-Walker T, Gal A, Weller AH, Li X, Fox JG, et al. Nitric oxide production in relation to spontaneous B-cell lymphoma and myositis in SJL mice. Cancer Res 1995;55:4391–7.
18. Compton SA, Elmore LW, Haydu K, Jackson-Cook CK, Holt SE. Induction of nitric oxide synthase-dependent telomere shortening after functional inhibition of Hsp90 in human tumor cells. Mol Cell Biol 2006;26:1452–62.
19. Cannons JL, Karsh J, Birnboim HC, Goldstein R. HPRT$^-$ mutant T cells in the peripheral blood and synovial tissue of patients with rheumatoid arthritis. Arthritis Rheum 1998;41:1772–82.
20. Yamanishi Y, Boyle DL, Green DR, Keystone EC, Connor A, Zollman S, et al. p53 tumor suppressor gene mutations in fibroblast-like synoviocytes from erosion synovium and non-erosion synovium in rheumatoid arthritis. Arthritis Res Ther 2005;7: R12–8.
21. Baecklund E, Iliadou A, Askling J, Ekbom A, Backlin C, Granath F, et al. Association of chronic inflammation, not its treatment, with increased lymphoma risk in rheumatoid arthritis. Arthritis Rheum 2006;54:692–701.
22. Schonland SO, Lopez C, Widmann T, Zimmer J, Bryl E, Goronzy JJ, et al. Premature telomeric loss in rheumatoid arthritis is genetically determined and involves both myeloid and lymphoid cell lineages. Proc Natl Acad Sci U S A 2003;100:13471–6.
23. Olson RR, Reuter JJ, McNicholl J, Alber C, Klohe E, Callahan K, et al. Acidic residues in the DR β chain third hypervariable region are required for stimulation of a DR(α, β 1*0402)-restricted T-cell clone. Hum Immunol 1994;41:193–200.
24. Holoshitz J, Vila LM, Keroack BJ, McKinley DR, Bayne NK. Dual antigenic recognition by cloned human $\gamma\delta$ T cells. J Clin Invest 1992;89:308–14.
25. Koizumi H, Liu CC, Zheng LM, Joag SV, Bayne NK, Holoshitz J, et al. Expression of perforin and serine esterases by human γ/δ T cells. J Exp Med 1991;173:499–502.
26. Day CL, Seth NP, Lucas M, Appel H, Guathier L, Lauer GM, et al. Ex vivo analysis of human memory CD4 T cells specific for hepatitis C virus using MHC class II tetramers. J Clin Invest 2003;112:831–42.
27. Pumpens P, Grens E. Hepatitis B core particles as a universal display model: a structure-function basis for development. FEBS Lett 1999;442:1–6.
28. Borisova G, Borschukova O, Skrastina D, Dislers A, Ose V, Pumpens P, et al. Behavior of a short preS1 epitope on the surface of hepatitis B core particles. Biol Chem 1999;380:315–24.
29. Bronte V, Serafina P, De Santo C, Marigo I, Tosello V, Mazzoni A, et al. IL-4-induced arginase 1 suppresses alloreactive T cells in tumor-bearing mice. J Immunol 2003;170:270–8.
30. Hegardt P, Widegren B, Sjogren HO. Nitric-oxide-dependent systemic immunosuppression in animals with progressively growing malignant gliomas. Cell Immunol 2000;200:116–27.
31. Pope RM. Apoptosis as a therapeutic tool in rheumatoid arthritis. Nat Rev Immunol 2002;2:527–35.
32. Mountz JD, Hsu HC, Matsuki Y, Zhang HG. Apoptosis and rheumatoid arthritis: past, present and future directions. Curr Rheum Rep 2001;3:70–8.
33. Carding SR, Egan PJ. $\gamma\delta$ T cells: functional plasticity and heterogeneity. Nat Rev Immunol 2002;2:336–44.
34. Bank I, Cohen L, Mouallem M, Farfel Z, Grossman E, Ben-Nun A. $\gamma\delta$ T cell subsets in patients with arthritis and chronic neutropenia. Ann Rheum Dis 2002;61:438–43.
35. Holoshitz J. Activation of $\gamma\delta$T cells by mycobacterial antigens in rheumatoid arthritis. Microbes Infect 1999;1:197–202.
36. Hajeer AH, Worthington J, Silman AJ, Ollier WE. Association of tumor necrosis factor microsatellite polymorphisms with HLA–DRB1*04–bearing haplotypes in rheumatoid arthritis patients. Arthritis Rheum 1996;39:1109–14.
37. Bodinier M, Peyrat MA, Tournay C, Davodeau F, Romagne F, Bonneville M, et al. Efficient detection and immunomagnetic sorting of specific T cells using multimers of MHC class I and peptide with reduced CD8 binding. Nat Med 2000;6:707–10.
38. Boytim ML, Lyu SC, Jung R, Krensky AM, Clayberger C. Inhibition of cell cycle progression by a synthetic peptide corresponding to residues 65-79 of an HLA class II sequence: functional similarities but mechanistic differences with the immunosuppressive drug rapamycin. J Immunol 1998;160:2215–22.
39. Brown JH, Jardetzky TS, Gorga JC, Stern LJ, Urban RG, Strominger JL, et al. Three-dimensional structure of the human class II histocompatibility antigen HLA-DR1. Nature 1993;364: 33–9.
40. Gleimer M, Parham P. Stress management: MHC class I and class I-like molecules as reporters of cellular stress. Immunity 2003;19: 469–77.
41. Brooks AG, Boyington JC, Sun PD. Natural killer cell recognition of HLA class I molecules. Rev Immunogenetics 2000;2:433–48.
42. Bennett MJ, Lebron JA, Bjorkman PJ. Crystal structure of the hereditary haemochromatosis protein HFE complexed with transferrin receptor. Nature 2000;403:46–53.
43. Loconto J, Papes F, Chang E, Stowers L, Jones EP, Takada T, et al. Functional expression of murine V2R pheromone receptors involves selective association with the M10 and M1 families of MHC class Ib molecules. Cell 2003;112:607–18.
44. Klareskog L, Stolt P, Lundberg K, Kallberg H, Bengtsson C, Grunewald J, et al. A new model for an etiology of rheumatoid arthritis: smoking may trigger HLA–DR (shared epitope)–restricted immune reactions to autoantigens modified by citrullination. Arthritis Rheum 2006;54:38–46.
45. Silman AJ, MacGregor AJ, Thomson W, Holligan S, Carthy D, Farhan A, et al. Twin concordance rates for rheumatoid arthritis: results from a nationwide study. Br J Rheumatol 1993;32:903–7.
46. Hmadcha A, Bedoya FJ, Sobrino F, Pintado E. Methylation-dependent gene silencing induced by interleukin 1β via nitric oxide production. J Exp Med 1999;190:1595–604.
47. Wachsman JT. DNA methylation and the association between genetic and epigenetic changes: relation to carcinogenesis. Mutat Res 1997;375:1–8.
48. Fulop T Jr, Larbi A, Dupuis G, Pawelec G. Ageing, autoimmunity and arthritis: perturbations of TCR signal transduction pathways with ageing: a biochemical paradigm for the ageing immune system. Arthritis Res Ther 2003;5:290–302.
49. Gorman JD, Lum RF, Chen JJ, Suarez-Almazor ME, Thomson G, Criswell LA. Impact of shared epitope genotype and ethnicity on erosive disease: a meta-analysis of 3,240 rheumatoid arthritis patients. Arthritis Rheum 2004;50:400–12.
50. Van der Helm-van Mil AH, Huizinga TW, Schreuder GM, Breedveld FC, de Vries RR, Toes RE. An independent role of protective HLA class II alleles in rheumatoid arthritis severity and susceptibility. Arthritis Rheum 2005;52:2637–44.